

Con nement induced instability of thin elastic film

By Animangsu Ghatak¹ y

¹ Department of Chemical Engineering, Indian Institute of Technology, Kanpur,
UP 208016, India

A con ned incompressible elastic film does not deform uniformly when subjected to adhesive interfacial stresses but with undulations which have a characteristic wavelength scaling linearly with the thickness of the film. In the classical peel geometry, undulations appear along the contact line below a critical film thickness or below a critical curvature of the plate. Perturbation analysis of the stress equilibrium equations shows that for a critically con ned film the total excess energy indeed attains a minimum for a finite amplitude of the perturbations which grow with further increase in the con nement.

Keywords: Con nement, Incompressibility

1. Introduction

Spontaneous surface and interfacial instabilities of thin liquid films have been studied in different contexts, e.g. the classical Saffman-Taylor (Saffman et al 1958) problem in a Hele Shaw cell in which flow driven fingering patterns develop at the moving interface of two viscous or viscoelastic liquids (Hommes et al 1981, Nittmann et al 1985); disjoining pressure induced rupturing and dewetting (Reiter et al 1992, Sharma et al 1998) of ultra thin viscous films; spiral instabilities in viscometric flow of a viscoelastic liquid (Muller et al 1989, McKinley et al 1995); and fingering instability and cavitation during peeling a layer of viscoelastic adhesive (Fields et al 1976, Uthama et al 1989). While most of these viscous and viscoelastic systems have been well characterized experimentally and theoretically, similar surface undulations of con ned thin elastic films pose a different kind of problem despite geometric commonalities with many of the liquid systems. The essential difference being that unlike in the liquid system there is no flow of mass and consequent permanent deformation in the elastic body, where the extent of deformation is governed by the equilibrium of the external surface or body forces on the material and the elastic forces developed.

The specific system that will be described in this paper is a thin layer of elastic adhesive con ned between a rigid and a flexible plate. While the film remains strongly bonded to the rigid substrate, the flexible plate is detached from it in the classical peel geometry. High aspect ratio of such systems is noteworthy as the lateral length scale far exceeds the thickness of the film resulting in high degree of con nement for the adhesive. As a result, adhesive stresses at the interface does not always result in uniform deformation throughout the whole area of contact,

y To whom correspondence should be addressed; (aghatak@iitk.ac.in)

rather spatially varying deformations (Gent et al 1958, Gent et al 1969, Ghatak et al 2000, Monch et al 2001) attain lower energy for the system. Experimentally we see the existence of a critical thickness of the film or a critical curvature of the flexible plate below which the contact line between the film and the flexible plate does not remain straight, but turns undulatory with a characteristic wavelength which increases linearly with the thickness of the film (Ghatak et al 2003). While experimentally this phenomenon has been characterized, there is not much understanding as what drives this instability in a non-flow purely elastic system and how does the curvature of the plate or the thickness of the film result in critical conformation of the film. Here I present a perturbation analysis which addresses these questions highlighting the dual effects of the incompressibility of the elastic film and its conformation.

2. Problem Formulation

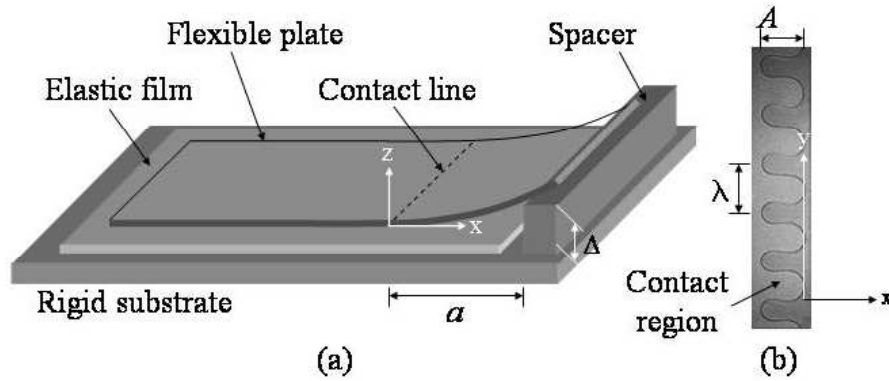


Figure 1. (a) Schematic of the experiment in which a model elastic adhesive remains bonded to a rigid substrate and a flexible plate is detached from it with the help of a spacer inserted at the opening of the crack. For a critically conformed film, the contact line does not remain smooth but becomes undulatory as shown in video-micrograph (b).

The schematic of our experiment is represented in Figure 1a in which an elastic film of thickness h and shear modulus μ remains strongly bonded to a rigid substrate while a flexible plate of rigidity D in contact with the film in the form of a curved elastica is supported at one end using a spacer of height Δ . The straight contact line between the film and the plate becomes wavy when the film thickness h decreases below a critical value h_c or the curvature of the plate decreases below a critical value $1/\rho = \rho_c$. Figure 1b represents a typical video-micrograph of such undulations which are characterized by two different length scales: the separation distance between the waves which scales as $4h$ and the amplitude A which varies with D and a as: $A \propto (D/a)^{1/3}$ (Ghatak et al 2003). The figure depicts also the co-ordinate system in which x , y and z axes represent respectively the direction of propagation of the contact line, the direction of the wave vector and the thickness coordinate of the film. The y axis is located along the tips of the waves so that the film is completely out of contact with the plate at $0 < x < a$. Assuming the film to be incompressible and purely elastic with no viscous effect, we write the following stress equilibrium

relations in the absence of any body forces,

$$\begin{aligned} p_x &= (u_{xx} + u_{yy} + u_{zz}) \\ p_y &= (v_{xx} + v_{yy} + v_{zz}) \\ p_z &= (w_{xx} + w_{yy} + w_{zz}) \end{aligned} \quad (2.1)$$

where, u, v and w are the displacements in the x, y and z directions respectively and p is the pressure. Here and everywhere $s_x = \partial s / \partial x$ and $s_{xx} = \partial^2 s / \partial x^2$. The incompressibility of the lm results in:

$$u_x + v_y + w_z = 0 \quad (2.2)$$

These equations are solved using the following set of boundary conditions (b.c.):

(a) since the lm remains strongly bonded to the substrate we use no slip boundary condition at the interface of the lm and the substrate ($z = 0$),

$$u(z = 0) = v(z = 0) = w(z = 0) = 0 \quad (2.3)$$

(b) we assume frictionless contact at the interface of the lm and the cover plate, $z = h$ which results in zero shear stress at the interface,

$$x_z(x; y; h) = 0 = y_z(x; y; h) \quad (2.4)$$

(c) we assume continuity of normal stress across the interface ($z = h$) which implies that the pressure is equal to the bending stress on the plate

$$p(z = h) = D r^2(z = h) \quad \text{at } x < 0 \quad (2.5)$$

here $r^2 = \partial^2 / \partial x^2 + \partial^2 / \partial y^2$ is the two dimensional Laplacian, D is the flexural rigidity of the plate and $w|_{z=h}$ is its vertical displacement. Since the plate bends only in the direction of x co-ordinate its vertical displacement remains uniform along the y axis; hence, we simplify b.c. 2.5 as

$$p(z = h) = D w_{xxxx}(z = h) \quad \text{at } x < 0 \quad (2.6)$$

At $0 < x < a$ there is no traction either on the lm or the plate which yields

$$x_z|_{z=h} = y_z|_{z=h} = z_z|_{z=h} = 0 \quad (2.7)$$

Equation (2.1)-2.2 can be written in dimensionless form using the following dimensionless quantities,

$$X = x/q; Y = y/h; Z = z/h; U = u/q; V = v/h; W = w/h; \theta = \theta/h; P = p/q^2 =$$

While thickness h of the lm is the characteristic lengths along the y and z axes, q^{-1} is that along x . The length q^{-1} can be derived as the ratio of the deformability of the plate and the lm (Dillard et al 1989, Ghatak et al 2004): $q^{-1} = D h^3 / 3 \mu = 6$. The quantity $\theta = h/q$ defined as the ratio of the two characteristic lengths is a measure of the con nement of the lm such that a lower value of θ represents a more con ned lm. Equations 2.1 and 2.2 can then be written in the following dimensionless form

$$\begin{aligned} P_X &= U_{XXX} - U_{YY} + U_{ZZ} \\ P_Y &= V_{XXX} + V_{YY} + V_{ZZ} \\ P_Z &= W_{XXX} + W_{YY} + W_{ZZ} \\ 0 &= U_X + V_Y + W_Z \end{aligned} \quad (2.8)$$

while the boundary conditions 2.3-2.7 results

$$\begin{aligned}
 (a) \quad & U(Z=0) = V(Z=0) = 0 \\
 (b) \quad & \frac{\partial U}{\partial Z}(X;Y;Z=1) = 0 = \frac{\partial V}{\partial Z}(X;Y;Z=1) \\
 (c) \quad & P(Z=1) = 3 \frac{\partial^2 U}{\partial X^2} \text{ at } X < 0 \\
 (d) \quad & 0 = \frac{\partial^2 U}{\partial X^2} \text{ at } 0 < X < aq \quad (2.9)
 \end{aligned}$$

where aq is the dimensionless crack length. Equation 2.8 is solved by the regular perturbation technique which assumes that the solutions consist of two components: the base solutions which remain uniform along the Y co-ordinate and the correction term which incorporates the spatial variation along the Y axis. Thus the base solutions are of order 0 and the perturbed solutions are of order $2; 4; \dots$, so that any variable $T(X;Y;Z) = T_0(X;Z) + \epsilon^2 T_1(X;Y;Z) + \epsilon^4 T_2(X;Y;Z) + \dots$ where $T = P, U, V$ and W . Inserting these definitions in equation 2.8 and separating the base (Y independent) and the perturbed (Y dependent) terms yield:

$$P_{0X} = \epsilon^2 U_{0XX} + U_{0ZZ}; \quad P_{0Z} = \epsilon^4 W_{0XX} + \epsilon^2 W_{0ZZ}; \quad 0 = U_{0X} + W_{0Z} \quad (2.10)$$

and

$$\begin{aligned}
 \epsilon^2 P_{1X} + \epsilon^4 P_{2X} &= \epsilon^2 (U_{1YY} + U_{1ZZ}) + \epsilon^4 (U_{1XX} + U_{2YY} + U_{2ZZ}) + \epsilon^6 U_{2XX} \\
 \epsilon^2 P_{1Y} + \epsilon^4 P_{2Y} &= \epsilon^4 (V_{1YY} + V_{1ZZ}) + \epsilon^6 (V_{1XX} + V_{2YY} + V_{2ZZ}) \\
 \epsilon^2 P_{1Z} + \epsilon^4 P_{2Z} &= \epsilon^4 (W_{1YY} + W_{1ZZ}) + \epsilon^6 (W_{1XX} + W_{2YY} + W_{2ZZ}) \\
 0 &= U_{1X} + V_{1Y} + W_{1Z} \quad (2.11)
 \end{aligned}$$

which are solved using b.c. derived from equations 2.9a-d.

Base Solution: Since for a thin film, $\epsilon^2 \ll 1$, equation 2.10 can be simplified by neglecting the terms containing ϵ^2 . Integration of the resulting equations (presented in detail in reference Ghatak et al 2004) finally leads to the following solution for the base components of the displacements in the film and the plate,

$$\begin{aligned}
 U_0 &= \frac{3Z^2}{2} - \frac{3Z}{2} F_0^0(X); \quad W_0 = \frac{3Z^2}{2} - \frac{Z^3}{2} F_0^0(X) \\
 P_1 &= e^{X/2} aq e^{X/2} + (3aq + 4) \sin \frac{P_1}{3X} = \frac{P_1}{3} aq \cos \frac{P_1}{3X} \\
 P_2 &= e^{X/2} aq e^{X/2} + (3aq + 2) \sin \frac{P_2}{3X} = \frac{P_2}{3} + (aq + 2) \cos \frac{P_2}{3X} \\
 F_0^0 &= \frac{3}{2} = \frac{6}{3} + 12aq + 9(aq)^2 + 2(aq)^3 \\
 P_0 &= F_0^0(X) \quad X < 0 \\
 &= F_0^0 \frac{2}{3} (aq + 1) + (3aq + 2)X + aqX^2 \quad X^3 = 3 \quad 0 < X < aq \quad (2.12)
 \end{aligned}$$

which suggest oscillatory variation along X with exponentially vanishing amplitude away from the contact line. Such displacements results in the following expression for the dimensionless work of adhesion (Ghatak et al 2004) $G = W_A (=q)$:

$$\begin{aligned}
 G &= g(aq) - \frac{27}{2} aq^4 \\
 g(aq) &= \frac{8}{3} aq^4 - 12 + 46(aq) + 72(aq)^2 + 56(aq)^3 + 21(aq)^4 + 3(aq)^5 = \\
 &\quad \frac{3}{2} - 6 + 12(aq) + 9(aq)^2 + 2(aq)^3 \quad (2.13)
 \end{aligned}$$

in which $g(aq)$ is the correction to the classical result of Obreim o (Obreim o et al 1930) for peeling o a rigid substrate.

Perturbation Analysis: Matching the coefficients for i , $i = 2, 4$ in the left and the right hand side of equation 2.11 results in the following set of equations:

$$\begin{aligned} 2: P_{1X} &= U_{1YY} + U_{1ZZ}; & P_{1Y} &= 0; & P_{1Z} &= 0 \\ 4: P_{2X} &= U_{1XX} + U_{2YY} + U_{2ZZ}; & P_{2Y} &= V_{1YY} + V_{1ZZ}; & P_{2Z} &= W_{1YY} + W_{1ZZ} \\ & U_{1X} + V_{1Y} + W_{1Z} & & & & = 0 \end{aligned} \quad (2.14)$$

we assume also that the excess quantities vary sinusoidally along the Y axis: so that $T_i = T_i \sin(KY)$; $T = U, V, W, P$; $i = 1, 2$; $K = 2\pi/\lambda$ is the dimensionless wave number of the perturbed waves. Equations 2.14 are solved using the following boundary conditions derived from 2.9,

$$\begin{aligned} (a) \text{ at } Z = 0 & \quad U_1 = V_1 = W_1 = U_2 = 0 \\ (b) \text{ at } Z = 1 & \quad U_{1Z} = 0 \quad U_{2Z} + W_{1X} = 0 \quad V_{1Z} + W_{1Y} = 0 \\ (c) \text{ at } Z = 1; X < 0 & \quad P_1 = 3\sigma_{1XX}; \quad \text{at } 0 < X < aq \quad 0 = \sigma_{1XX} \end{aligned} \quad (2.15)$$

where $W_1(X; Z = 1)$ is the vertical displacement of the flexible plate at $Z = 1$. Assumption of sinusoidal dependence on Y is a simplification which is apparent from the video micrographs of the contact line as in figure 1b which show that the film and the plate remains in contact whole through the area of the finger implying that the deformation of the film is not perfectly sinusoidal, as it would mean a line contact between the plate and the film. However, here I assume sinusoidal variation to keep the calculations simple. Since, the plate does not bend in the direction of Y , σ_{1X} and σ_{1XX} both remain uniform along this axis; consequently in b.c. 2.15c, bending stress on the plate is equated to P_1 . Equation 2.14 suggests that P_1 remains independent of Y and Z although U_1 varies along Y , hence, the only solution for P_1 that can satisfy equation 2.14 is $P_1 = 0$. Other components of the excess displacements are obtained as:

$$\begin{aligned} U_1 &= 0 \\ V_1 &= \frac{C(X)}{K} \frac{2K e^K + e^K}{e^K + e^K + 2K e^K} \sinh(KZ) + \\ & \quad KZ \frac{e^K + e^K}{e^K + e^K + 2K e^K} e^{KZ} e^{KZ} \cos(KY) \\ W_1 &= \frac{C(X)}{K} \frac{2e^K + 2e^K + 2K e^K}{e^K + e^K + 2K e^K} \sinh(KZ) + \\ & \quad KZ \frac{e^K + e^K}{e^K + e^K + 2K e^K} e^{KZ} + e^{KZ} \sin(KY) \end{aligned} \quad (2.16)$$

Here, only the lowest order terms in ϵ are computed since the higher order terms enhance accuracy insignificantly. Since for all our experiments, $\epsilon < 0.3$, the above solutions imply that the excess deformations in the film occur under very small excess pressure which is of the order $\epsilon^4 < 0.01$. This excess pressure, however small, varies along Y implying that it should depend upon the distance between the plate and the film. Nevertheless, the excess traction which results from the

distance dependent forces (Shenoy et al 2001, Sarkar et al 2004) apply only in the immediate vicinity ($< 0.1 \text{ nm}$) of the contact between the film and the plate as the gap between the two increases rather sharply (could be observed in AFM images of the permanent patterns of surface undulations). Hence, it does not contribute any significantly to the overall energetics.

While equation 2.16 elaborates the variation of excess deformations along Y and Z , their dependence on X is incorporated through the coefficient $C(X)$ which is obtained by solving equations 2.15c using the following boundary conditions

$$\begin{aligned} \text{(i, ii)} \quad w|_{X=0} &= C_0(K) & \text{(iii)} \quad \frac{dw}{dX}|_{X=0} &= \frac{dw}{dX}|_{X=0+} \\ \text{(iv)} \quad \frac{d^2w}{dX^2}|_{X=0} &= \frac{d^2w}{dX^2}|_{X=0+} & \text{(v, vi)} \quad \frac{d^3w}{dX^3}|_{X=a} &= \frac{d^3w}{dX^3}|_{X=a+} = 0 \\ \text{(vii, viii)} \quad \frac{d^4w}{dX^4}|_{X=a} &= \frac{d^4w}{dX^4}|_{X=a+} = 0 \end{aligned}$$

Where, $a = Aq$ is the dimensionless amplitude of the waves and $C_0(K)$ is the excess stretching of the film at $x = 0$: C_0 is a constant and $C(K) = W_1 = C(X)|_{X=0} = e^{-K} - e^{-3K} + 4K e^{-K} = K[1 + e^{2K}(1 + 2K)]$. (a) B.C. i, ii, iii and iv occur because the excess displacement and slope of the plate are continuous at $X = 0$; (b) at $X = a$ the displacement of the plate, its slope should vanish, which result in the b.c. v and vi; (c) similarly, at $X = aq$ excess displacement and curvature of plate is zero, which results in b.c. vii and viii. Incorporating these boundary conditions into the solutions of equations 2.15c yield the following expression for the the excess displacement of the plate:

$$\begin{aligned} w_1 &= \frac{C_0(K)}{aq(3 + 4aq)} \left[\frac{3}{2} X^2 + 6aqX + 2(aq)^2 \right] (X = 0)^3 - \frac{3}{2} X^2 + 3aqX (X = a)^2 \\ &\quad - \frac{3}{2} X^2 - 2(aq)^2 X (X = a) + aq(3 + 4aq) \quad \text{at } X < 0 \\ w_1 &= C_0(K) \left[1 + \frac{aq}{(3 + 4aq)} (2 + 3aq) \right] (X = aq)^3 \\ &\quad - \frac{3}{2} (2 + 3aq) (X = aq)^2 - \frac{3}{2} X^2 - 2(aq)^2 X = (aq)^2 \quad \text{at } 0 < X < aq \quad (2.17) \end{aligned}$$

Excess Energy: Total energy of the system consists of the elastic energy of the film, bending energy of the plate and the interfacial energy:

$$\begin{aligned} &= \int_0^a \int_0^b \int_{-\infty}^{\infty} \left[\frac{1}{2} \left(\frac{\partial w}{\partial x} \right)^2 + \frac{1}{2} \left(\frac{\partial w}{\partial y} \right)^2 + \frac{1}{2} \left(\frac{\partial w}{\partial z} \right)^2 \right] dz dy dx \\ &= \frac{1}{4} \int_0^a \int_0^b \left[\left(\frac{\partial w}{\partial x} \right)^2 + \left(\frac{\partial w}{\partial y} \right)^2 + \left(\frac{\partial w}{\partial z} \right)^2 \right] dz dy dx \\ &\quad + \frac{D}{2} \int_0^a \int_0^b \left(\frac{\partial^2 w}{\partial x^2} \right)^2 dy dx + W_A (2ab + A_{\text{inter}}) \quad (2.18) \end{aligned}$$

where A_{inter} is the interfacial area of contact at $-a < x < 0$. From equation 2.18 the excess energy of the system is obtained as $E_{\text{excess}} = E_0$ which is written in a dimensionless form using E_0 as the characteristic energy and by substituting for variables $T = T_0 + T_1 + T_2$, where $T = U, V, W$ and P .

The expression for excess elastic energy e in the ln is obtained as,

$$e = \frac{1}{4} \int_0^Z \int_0^{2\pi K} \int_0^1 \left[{}^6 V_{1Z} + W_{1Y} + {}^2 (V_{2Z} + W_{2Y})^2 + {}^8 U_{2Y} + V_{1X} + {}^2 V_{2X}^2 + {}^8 (U_{2Z} + W_{1X}) + {}^2 W_{2X}^2 + {}^2 {}^4 U_{0Z} + {}^2 W_{0X} U_{2Z} + W_{1X} + {}^2 W_{2X} \right] dZ dY dX \quad (2.19)$$

where I estimate the excess energy within a distance $X = 0$. Considering only the leading order terms (4 and 6) I can simplify the expression in 2.19 as,

$$e = \frac{{}^6}{4} \int_0^Z \int_0^{2\pi K} \int_0^1 (V_{1Z} + W_{1Y})^2 dZ dY dX \quad (2.20)$$

in which I substitute the expressions for V_1 and W_1 from 2.16 to obtain

$$e = {}^6 C_0^2 f_2(\gamma; aq; K) = {}^6 C_0^2 f_0(K) f_2(\gamma; aq) = 4 \quad (2.21)$$

Similarly, the dimensionless excess bending energy b of the plate:

$$b = (3 = K) \int_0^Z \int_0^{2\pi K} \int_0^1 \left[{}^2 {}^2 {}_0 X X + {}_1 X X + {}^4 {}_1 X X + {}^2 {}_2 X X^2 \right] dX \quad (2.22)$$

Considering only the leading order terms: 2 and 4 , equation 2.22 simplifies to

$$b = \frac{3}{K} \int_0^Z \int_0^{2\pi K} \int_0^1 \left[{}^2 {}^2 {}_0 X X + {}_1 X X + {}^4 {}_1 X X \right] dX \quad (2.23)$$

Substituting the expressions for ${}_0$ and ${}_1$ from 2.12 and 2.17, b is obtained as,

$$b = {}^2 C_0 f_3(\gamma; aq; K) + {}^4 C_0^2 f_1(\gamma; aq; K) \quad (2.24)$$

The interfacial energy is estimated as,

$$i = 2G \int_0^Z \int_0^{2\pi K} \frac{1}{2} \sin(KY) dY = \frac{2G}{K} \quad (2.25)$$

Substituting the expression for G from equation 2.13 in equation 2.25 and combining all the three energies, yields the total excess energy as:

$$= {}^6 f_2(\gamma; aq; K) + {}^4 f_1(\gamma; aq; K) C_0^2 + {}^2 f_3(\gamma; aq; K) C_0 + \frac{27}{K} \frac{g(aq)}{(aq)^4} \quad (2.26)$$

The expressions for $f_1(\gamma; aq; K)$, $f_2(\gamma; aq; K)$ and $f_3(\gamma; aq; K)$ are obtained using Mathematica and are not being presented here since they could not be written in a compact form.

3. Results and Discussion

The expression for excess energy in equation 2.26 accounts for the combined effects of three sets of parameters: γ , the con nement parameter, aq and K , the characteristic length scale of the perturbations and aq and γ , the length scale of the geometry

of the experiment. In what follows, we look for the solutions of these different sets of parameters which results in negative excess energy associated with the instability.

While it is evident from equation 2.26 that ϵ and K are nonlinearly coupled quantities, the physics of the problem is better understood if we study their effects separately. We do that following the observation that the excess displacements in the film but not that of the plate are functions of Y , which allows us to assume that the dimensionless wave number K of the perturbations is determined solely by the minimum of the excess elastic energy ϵ_e and not the other components of the total excess energy. Although this assumption is not exactly correct as the displacement of the plate is also a function of K , experimental observation that the amplitude remains nearly independent of the wavelength (Ghatak et al 2003) suggests that the above assumption should not insert much inaccuracy into the calculation.

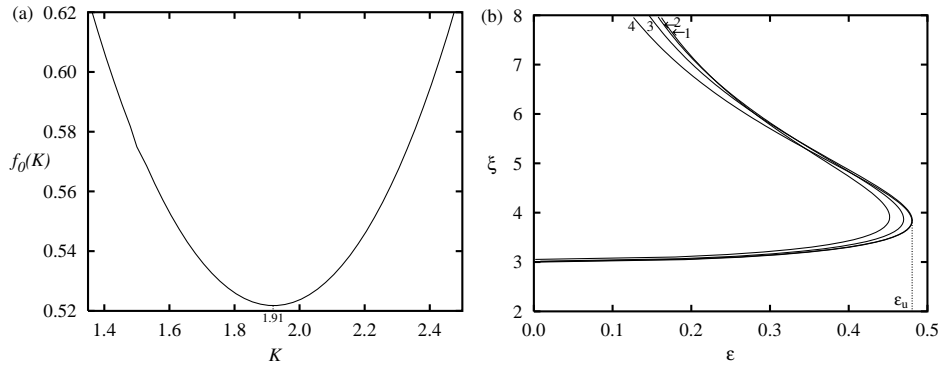


Figure 2. (a) Dimensionless elastic energy of the film is plotted against the dimensionless wave number K of the surface undulations. The energy of the film attains a minimum at $K = 1.91$ implying that the wavelength varies with thickness of the film as $\lambda = 3.3h$. (b) Amplitude ξ are plotted against the limiting values of ϵ from equation 3.2 for different values of the dimensionless length aq . Curves 1-4 represent $aq = 5, 15, 25$ and 55 respectively. $\epsilon_u = 0.48$ is the upper limit for ϵ beyond which no real solution for C_0 exists.

The plot of excess elastic energy ϵ_e vs. the wave number K in figure 2a then shows that ϵ_e attains a minimum when $K = 1.91$. The wavelength of perturbations thus scales with the thickness of the film as $\lambda = 3.3h$ which corroborates with the general observation in a wide range of experimental geometries (Ghatak et al 2000, 2003, Monch et al 2001) that λ remains independent of all the material and the geometric properties of the system except h . Furthermore, the proportionality constant matches well with that observed in experiments ($\lambda = 3.4h$) with rigid and flexible contacting plates.

Although the minimum of ϵ_e occurs at $K = 1.91$ irrespective of C_0 and ϵ , for both these parameters real values are desired. In fact, equation 2.26, being quadratic w.r.t. C_0 , suggests that in the limit $\epsilon = 0$ the real solutions for C_0 exist only when,

$$2f_3(\epsilon; aq; K)^2 - 4\epsilon^6 f_2(\epsilon; aq; K) + 4f_1(\epsilon; aq; K)(27 - K)g(aq) = (aq)^4 \quad (3.1)$$

resulting in the following inequality for ϵ^2 :

$$\epsilon^2 \geq \frac{f_3^2(\epsilon; aq; K) K}{4f_2(\epsilon; aq; K) 27} \frac{(aq)^4}{g(aq)} \frac{f_1(\epsilon; aq; K)}{f_2(\epsilon; aq; K)} \quad (3.2)$$

Equation 3.2 sets an upper bound for ξ as evident from gure 2b where ξ_i and ξ_{min} which satisfy equation 3.2 are plotted for $K = 1.91$ and for di erent aq . When ϵ is smaller than this upper critical limit ξ_c , two di erent solutions for ξ exist, the stability of which depends upon whether Π attains a minimum at these solutions. Hypothesizing that Π minimizes when $\partial \Pi / \partial \xi = 0$, we obtain an expression for C_0 which when substituted in 2.26, yields

$$C_0 = \frac{2}{4} \frac{f_3(\epsilon; aq; K)^2}{f_1(\epsilon; aq; K) + 2f_2(K; \epsilon)} + \frac{27}{K} g(aq) \quad (3.3)$$

In gure 3a we plot Π/Δ^2 from equation 3.3 w.r.t. ξ , for $\epsilon = 0.48$ to 0.05. For all these

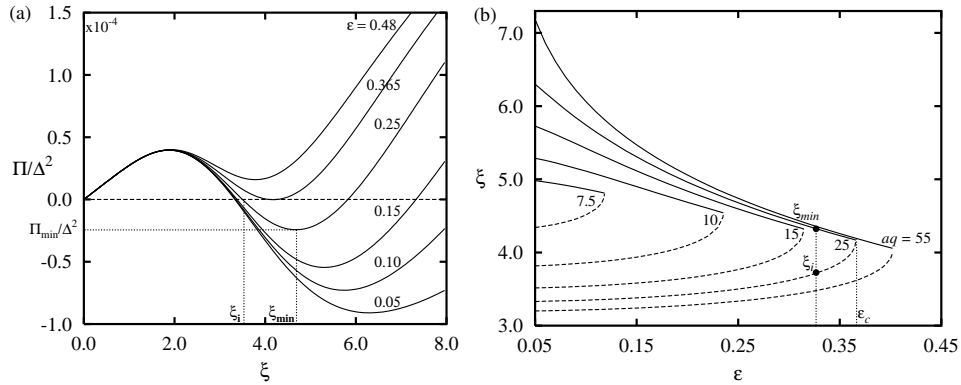


Figure 3. (a) Dimensionless excess energy Π is plotted against the dimensionless amplitude of the waves for di erent values of the confinement parameter ϵ . The curves are obtained using representative values for the dimensionless parameters: $aq = 25$, and $K = 1.91$. (b) Bifurcation diagram showing variation of ξ w.r.t. ϵ for di erent values of aq and $K = 1.91$. The dotted and the solid lines represent respectively ξ_i vs. ϵ and ξ_{min} vs. ϵ . No solution for ξ exists beyond ξ_c .

cases, Π exhibits a non-monotonic character: with increase in ξ , it first increases till it reaches a maximum after which it decreases to attain a minimum, thereafter it increases again. Stability of these systems is determined by the minimum of the excess energy which if positive signifies stable base solution for the contact line and unstable solution if negative. For example, for $\epsilon = 0.48$ remains positive all-through implying that the undulation of a straight contact line would increase the total energy of the system so that a straight contact line would remain stable. On the other hand, $\epsilon = 0.365$, presents a limiting case for which minimum of the excess energy Π_{min} attains zero and for $\epsilon = 0.25, 0.15, 0.1$ and 0.05 , Π_{min} becomes negative, i.e. when the lm is more than critically confined i.e. $\epsilon < \epsilon_c = 0.365$, the contact line can become unstable if sufficiently perturbed. The critical value $\epsilon_c = 0.365$ thus obtained for the above set of data corroborates well with 0.3 obtained in experiments of gure 1. Furthermore, a finite energy barrier at $\xi < \xi_i$ suggests that a straight contact line is not unstable for perturbations of all magnitude. Because, for perturbation with amplitude $\xi < \xi_i$ the excess energy remains positive so that these perturbations decay to zero. This result too corroborates with experiment that with increase in confinement of the lm, the amplitude of the undulations never

increases from exactly zero, but from a finite value. When $\epsilon > \epsilon_i$, ϵ decreases to become negative, so that these perturbations can grow till ϵ reaches ϵ_{min} , at which ϵ attains the minimum ϵ_{min} ; ϵ_{min} is then the predicted amplitude of the undulations of the contact line.

Figure 3b depicts the bifurcation diagram where ϵ_i (dashed line) and ϵ_{min} (solid line) are plotted with respect to ϵ for variety of aq . The dashed lines signify that the perturbations whose amplitude $< \epsilon_i$ decay to zero, whereas solid lines mean those with $> \epsilon_i$ grow to ϵ_{min} . The amplitude ϵ_{min} increases with increase in the con nem ent of the ϵ similar to that observed in experiments, although, the values predicted are somewhat (2-3 times) larger than what is observed. This discrepancy could be due to the underestimation of the excess elastic energy of the ϵ . In figure 4 the combined effects of ϵ and K are probed by plotting ϵ w.r.t.

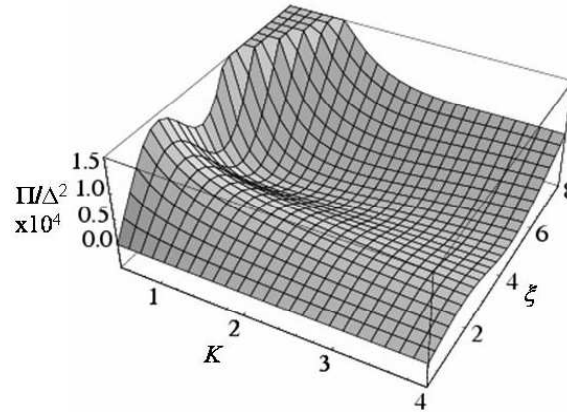


Figure 4. Excess energy ϵ for $\epsilon = 0.2$ and $aq = 25$ is plotted w.r.t amplitude ϵ and wave number K .

and K . Here again ϵ_{min} becomes negative for con nem ent parameter ϵ below a critical value $\epsilon_c = 0.365$. However, the wave number K at which the minimum occurs does not remain constant, it decreases from 2.12 to 0.5 while ϵ varies from 0.365 to 0.05. Although this prediction is somewhat different from experiments, in which ϵ varies between 0.3 to 0.1 at which K is observed to be 1.57 to 0.1, some recent observations (personal communication with Prof. A. Sharma) with very thin elastic ϵ s (0.5 μ m) indeed indicate that K can decrease to 1.0 as ϵ decreases to 0.07. More experiments are clearly necessary to characterize quantitatively the effect of the coupling of the two length scales with highly con ned elastic ϵ s.

4. Summary

The analysis shows that con nem ent of an incompressible elastic ϵ leads to favorable energetics for perturbations to grow so that the ϵ can not deform uniformly everywhere when subjected to the tensile stresses at the interface. Furthermore, the nature of the adhesion stress is not important, even the spatial variation of the surface forces play rather an insignificant role. While the theory captures the essential physics of the problem, slight overestimation of the amplitude possibly results from the assumption of sinusoidal variations along the Y axis which is not

perfectly correct. These issues can possibly be resolved by 3D simulation of the force field near the contact line. Nevertheless the results presented in this paper should be important for many other systems in confined geometries.

Acknowledgement: I sincerely thank Prof. M. K. Chaudhury in whose laboratory at Lehigh University and under whose guidance all experiments were carried out. I thank also Prof. L. Mahadevan for suggesting the perturbation analysis for solving the elasticity equations. Many thanks to Prof. Anutosh Sharma and Prof. V. Shankar for many stimulating discussions.

References

- Dillard, D. A. 1989 Bending of plates on thin elastomeric foundations. *J. Appl. Mech.*, 56, 382{386.
- Fields, R. J. & Ashby, M. F. 1976 Finger-like crack growth in solids and liquids. *Philos. Mag.* 33, 33{48.
- Gent, A. N. ; Lindley, P. B. 1958 Internal rupture of bonded rubber cylinders in tension. *Proc. R. Soc. London, Ser. A*, 195{205.
- Gent, A. N. and Tompkins, D. J. 1969 Nucleation and growth of gas bubbles in elastomers. *J. Appl. Phys.* 40, 2520-2525.
- Ghatak, A. ; Shenoy, V. ; Chaudhury, M. K. ; Sharma, A. 2000 Meniscus instability in thin elastic film. *Phys. Rev. Lett.* 85, 4329{4332.
- Ghatak, A. ; Chaudhury, M. K. 2003 Adhesion induced instability patterns in thin confined elastic film. *Langmuir* 19, 2621{2631.
- Ghatak, A. ; Mahadevan, L. ; Chaudhury, M. K. 2005 Measuring the work of adhesion between a soft confined film and a flexible plate. *Langmuir* web released on 11th January.
- Homay, G. M. 1981 Viscous fingering in porous media. *Annu. Rev. Fluid Mech.*, 19, 271{311.
- McKinley, G. H. ; Oztekin, A. ; Byars, J. ; Brown, R. A. 1985 Self-similar spiral instabilities in elastic flows between a cone and plate. *J. Fluid Mech.*, 285, 123{164.
- Monch, W. ; Herminghaus, S. 2001 Elastic instability of rubber films between solid bodies. *Europhys. Lett.* 53, 525{531.
- Muller, S. J. ; Larson, R. G. ; Shaqfeh, E. S. G. 1989 *Rheol. Acta.* 28, 499.
- Nittmann, J. ; Daccord, G. ; Stanley, H. E. 1985 Fractal growth of viscous fingers: quantitative characterization of a fluid instability phenomenon. *Nature* 314, 141{144.
- O'Brien, J. W. 1930 The splitting strength of mica. *Proc. Roy. Soc. Lond. ser. A*, 127, 290{297.
- Reiter, G. 1992 Dewetting of thin polymer films. *Phys. Rev. Lett.* 68, 75{78.
- Saman, P. G. ; Taylor, G. I. 1958 The penetration of a fluid into a porous medium or Hele-Shaw cell containing a more viscous liquid. *Proc. Roy. Soc. London, series A* 245, 312{329.
- Sarkar, J. ; Shenoy, V. ; Sharma, A. 2004 Patterns, forces and metastable pathways in debonding of elastic film. *Phys. Rev. Lett.* 93, 018302{018305.
- Sharma, A. and Khanna, R. 1998 Pattern formation in unstable thin liquid film. *Phys. Rev. Lett.* 81, 3463{3466.
- Shenoy, V. ; Sharma, A. 2001 Pattern formation in a solid film with interactions. *Phys. Rev. Lett.* 86, 119{122.
- Uthama, Y. 1989 Effect of peel load on Stringiness phenomena and peel speed of pressure sensitive Adhesive tape. *J. Adhes.* 31, 47{58.